Available online at www.sciencedirect.com
ScienceDirect
Catalysis Today 120 (2007) 407–412
CATALYSIS TODAY
www.elsevier.com/locate/cattod

Hydrogen storage on Li-doped single-walled carbon nanotubes: Computer simulation using the density functional theory

Jung Hyun Cho, Chong Rae Park *

Carbon Nanomaterials Design Laboratory, Hyperstructured Organic Materials Research Center (HOMRC) and School of Materials Science and Engineering, Seoul National University, Seoul 151-744, Republic of Korea

Available online 13 November 2006

Abstract

The first principal calculation based on the density functional theory was performed to investigate the hydrogen storage behavior of Li-doped single-walled carbon nanotubes (SWCNTs). It was found that, through Li-doping, two new adsorption sites for hydrogen molecules are created in addition to the inherent three adsorptive sites which are exterior, interior and interstitial regions of pristine SWCNTs: the first site (denoted 'region 1') is the nanotube's sidewall whose electronic distribution status is influenced by the doped Li atoms. The second site (denoted 'region 2') exists on the positively charged Li atoms which result from the transfer of electrons from the Li atoms to the SWCNTs. The calculations show that although the adsorption energy in region 1 increases somewhat, the adsorption behavior of hydrogen is marginally different from that of pristine SWCNTs. However, in region 2, at least three hydrogen molecules can be adsorbed by each charged Li-atom, and based on the maximum Langmuir coverage (of 0.55), 1.1 hydrogen molecules can be adsorbed onto each charged Li-atom. When this result is considered together with the effective specific surface area, the hydrogen storage capacities of Li-doped SWCNTs with the doping ratio of LiC_{15} are approximately 0.1 wt% in region 1 and 1.17 wt% in region 2 at 10 MPa and 300 K so that the total H_2 storage capability is 1.27 wt%, which agrees well with previously reported results.

Keywords: Hydrogen adsorption; Li-doped SWCNTs; QM calculation; Density functional theory

1. Introduction

The hydrogen fuel cell is nowadays a worldwide issue since it is considered to be the most promising solution that could dramatically decrease pollution and decelerate the depletion of fossil fuel resources. However, for practical purposes, particularly for vehicles equipped with hydrogen fuel cell, we have to find appropriate ways of storing a considerable amount of hydrogen in a container or adsorbent. Indeed, the U.S. Department of Energy (DOE) suggested that such an adsorbent should store 6.5 wt% of hydrogen and/or 62.5 kg/m^3 for actual automotive fuel cell applications.

Recently, large hydrogen uptakes by lightweight nanostructured carbon materials such as single-walled carbon nanotubes (SWCNTs) have attracted considerable experimental and theoretical attention [1–4]. For example, high-purity SWCNTs have been reported to adsorb ca. 8.0 wt% at temperatures of 80 K and pressures of over 100 bars [5]. However, since the actual application in automobiles requires working conditions of ambient temperature and roughly 1–100 bars, materials as such pristine SWCNTs that require either high pressures or very low temperatures or both for large amounts of H_2 uptake would have many limitations in their applications to actual automobiles. Moreover, many studies both experimental [6–9] and dealing with simulations [10,11] have indeed reported hydrogen storage capabilities of less than 1 wt% at room temperature for nanotubes synthesized and pretreated with a variety of methods.

Much effort has therefore been expended in finding more feasible adsorbents for hydrogen storage. For example, multi-walled carbon nanotubes (MWCNTs) doped with alkali metals, particularly with Li and K showed enhanced hydrogen storage capacities at ambient pressure and temperature [12–14]: in a dry hydrogen atmosphere, the adsorption is of 2.5 wt% for Li-doped MWCNTs and of 1.8 wt% for K-doped MWCNTs. To find possible contributing factors of such enhanced hydrogen adsorption capacities, several theoretical studies have devoted themselves to understanding the relationships between the

* Corresponding author. Tel.: +82 2 880 8030; fax: +82 2 885 1748.
E-mail address: crpark@snu.ac.kr (C.R. Park).

0920-5861/$ – see front matter
doi:10.1016/j.cattod.2006.09.027

components in hydrogen/alkali metal/nanotube systems [15–17]. However, Froudakis merely mentioned the possibility of enhanced adsorption by alkali atoms for K-doped SWCNTs [15]. Cabria et al. reported that the physisorption energy of hydrogen molecules near Li atoms on the Li-doped carbon nanotubes is twice as large as that of the pristine SWCNTs (4,4) which is attributable again to the charge transfer from the Li atoms to the graphitic surface around them. But they performed local density functional (LDA) calculations which are not adequate for the calculations of dispersion forces [16]. Thus, all the abovementioned works may somewhat help understand what might be happening within the hydrogen/alkali metal/SWCNTs systems, but do not explain how such a high adsorption energy can contribute, in quantitative terms, to the enhancement of the hydrogen adsorption capacities of SWCNTs. This implies that there still remains a need for a more systematic study of the hydrogen adsorption behavior on Li-doped SWCNTs (denoted Li-SWCNTs) in order to find more quantitative information. Therefore, we aimed herein at elucidating the role of lithium in improving the hydrogen storage capacity of carbon nanotubes by adopting (10,0) SWCNTs as a model material and the methodology of quantum mechanical (QM) calculations using general gradient approximation density functional theory (GGA-DFT). Through this approach, we could find the interaction energies between Li atoms and SWCNTs, the changes in the electron distributions, and the most effective adsorption sites. Also, we were able to calculate the hydrogen capacities of Li-SWCNTs based on Langmuir coverage together with the effective specific surface area of the modeled tubes.

2. Computational and theoretical details

The adsorption of hydrogen molecules on carbon materials is dominated by van der Waals forces and long-range attractive forces between separated molecules even in the absence of charges or permanent electric moments. In order to describe van der Waals interactions effectively, a fully non-local functional must be adopted since a local density functional is in principle not capable of describing this long-range, non-local correlation effect. Therefore, we used the first-principle calculations based on density functional theories (DFT) with the generalized gradient approximation (PW91) suggested by Perdew and Wang [18]. For the accurate calculation of the interaction energy of hydrogen molecules on Li-SWCNTs, the DFT employed here is combined with a double numerical plus polarization basis set (DNP) as is embodied in the Dmol^3 code [19,20]. The DNP basis set consists of two atomic orbitals for each occupied atomic orbital, being a polarization *d*-function on all non-hydrogen atoms and a polarization *p*-function on all hydrogen atoms. The standard DNP basis set is equivalent to 6-31G** which is an analytic basis set. In the calculations, we set the orbital cut-off distance as 4.4 Å and the energy convergence as 10^{-5} Ha. And the model carbon nanotubes were (10,0) SWCNTs with the diameter of 0.79 nm. All calculations were carried out using a periodically repeating 3D triclinic lattice cell. The lattice constants of *a* and *b* for the inner and outer adsorption areas of SWCNTs were decided to be in the range of negligible interaction energy between neighboring tubes, and for the interstitial adsorption area the inter-tube distance of 0.35 nm was found to be the most appropriate stable value. The geometry of both SWCNTs and Li-doped SWCNTs were fully optimized through energy minimization, and the single point energy calculations were used to find the physisorption energies of hydrogen molecules. The adsorption energy of hydrogen molecules on either pristine SWCNTs or Li-doped SWCNTs were calculated using Eq. (1):

$$E_{\text{adsorption}} = E(\text{host material} - \text{H}_2) - E(\text{host material}) - E(\text{H}_2) \quad (1)$$

The adsorption coverage (f) that is dependent on the change of adsorption energy was calculated on the assumption of Langmuir type coverage [21] using Eq. (2):

$$f = \frac{1}{1 + \exp((E_{\text{adsorption}} - \mu)/kT)} \quad (2)$$

Here, μ is the chemical potential of hydrogen gas, k the Boltzman constant, and T is the adsorption temperature. Eq. (2) can only be used assuming that Langmuir type monolayer adsorption and physisorption are valid. However, due to dispersion forces [22], the most stable position for an adsorbed molecule is situated with its center at a distance of about one molecular diameter from the surface as the attractive field rapidly diminishes at greater distance. This would indicate that the adsorption energy of the second layer of adsorbate molecules is almost negligible. Consequently, the adsorption at a temperature equal or greater than the boiling point of the adsorbate at a given pressure leads to the adsorption of a monolayer, which means that the Eq. (2) is applicable to our simulated model.

3. Results and discussion

3.1. Hydrogen storage on pristine SWCNTs

SWCNTs exist in the state of aggregated long crystalline bundles consisting of a few tubes to hundreds of individual nanotubes closely packed into a triangular lattice due to van der Waals interactions. This structure renders the pristine SWCNTs into having three adsorptive sites: exterior, interior and interstitial regions. Also, according to our preliminary calculations, the adsorption of hydrogen molecules perpendicular to hexagonal ring centers were the most favorable, although their energy differences when compared to other configurations perpendicular to a carbon atom is below 0.2 kcal/mol. Consequently, we considered only the adsorption of hydrogen molecules perpendicular to a hexagonal ring center in all calculations.

Fig. 1 shows that the adsorption energies on exterior and interior regions are in the range of −2.19 to −2.20 kcal/mol, while those on interstitial regions are −6.57 kcal/mol, which are three times higher than the others. The adsorption capability

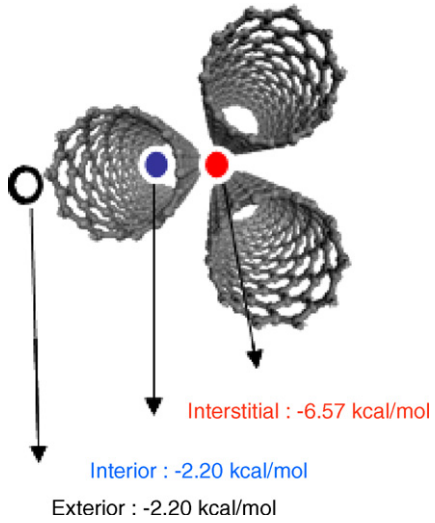

Fig. 1. Three adsorption regions and adsorption energies of the pristine single walled carbon nanotube.

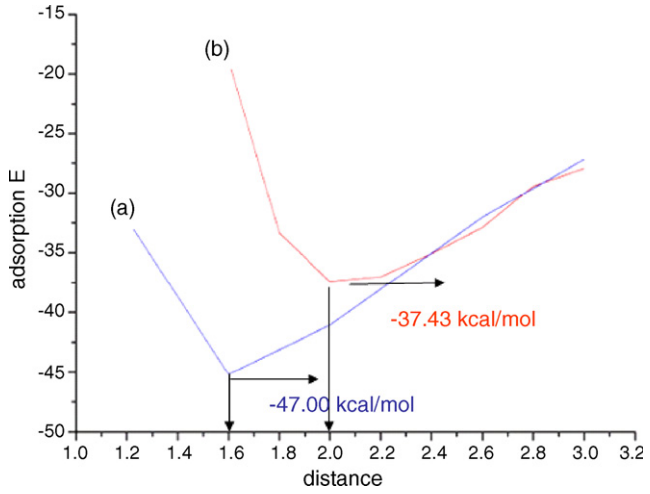

Fig. 3. The adsorption energy and the adsorption distance of Li atoms doped on pristine SWCNTs: (a) Li atoms doped on a hexagonal ring center of a SWCNT sidewall; (b) Li atoms doped on a carbon atom of a SWCNT's sidewall.

of the interior region differs slightly to that of the exterior region, but the difference is negligible when it is compared to the potential of the H_2 gas at room temperature. Also, the adsorption energy was almost the same for the various configurations of hydrogen molecules on SWCNTs. This result implies that the pristine SWCNTs do not have any specific adsorption site so that H_2 molecules can equally be adsorbed onto any region of the pristine SWCNTs wall. Consequently, if no impurities or disordered structures exist, the hydrogen adsorption sites in the pristine SWCNTs are limited to three regions: the interstitial, interior and exterior regions. Assuming that the Langmuir adsorption on pristine SWCNTs at 10 MPa and 300 K is valid, Eq. (2) yields the adsorption coverage of hydrogen at 0.85 wt% for the interstitial region and 0.02 wt% for the interior and exterior regions. This suggests that the hydrogen storage on the pristine SWCNTs is occurs mostly at the interstitial region. Fig. 2 illustrates the relationship between the hydrogen adsorption coverage and the adsorption energy.

As far as the hydrogen adsorption energy is concerned, SWCNTs is somewhat different from that of either flat or curved graphene layers which may be considered as reference adsorbents for SWCNTs: the adsorption energy for an isolated graphene layer was calculated to be −1.79 and −3.50 kcal/mol for the interlayer of the graphene sheets, which is much lower than the adsorption energies on SWCNTs. The effect of the curvature of graphene sheets on the adsorption of hydrogen can be neglected in this case, because the adsorption energy in the concave region is almost equal to that of the convex region. A question that arises immediately is why the adsorption energy of the pristine SWCNTs is larger than the adsorption energy of the graphene sheet. It is not easy at this stage to find a satisfactory answer to that question, but it seems it may have something to do with a different electron distribution status due to the structural differences between SWCNTs and the graphene sheet.

3.2. *Effect of Li-doping on pristine SWCNTs*

For the doped Li atoms located above a hexagonal ring center (Fig. 3a), the adsorption energy was calculated to be −47.00 kcal/mol and the adsorption distance was ca. 1.6 Å, while, for the doped Li located above a carbon atom (Fig. 3b), the adsorption energy was −37.43 kcal/mol and the adsorption distance of the SWCNTs was 2.0 Å. This indicates that doping occurs favorably over a hexagonal ring center of a SWCNT side wall. In order to see if there is any change in the electron density, we performed the Mulliken analysis (Fig. 4) for Li-SWCNTs. Fig. 4 clearly shows that there exist electron transfers from Li atoms to nanotubes although it is localized

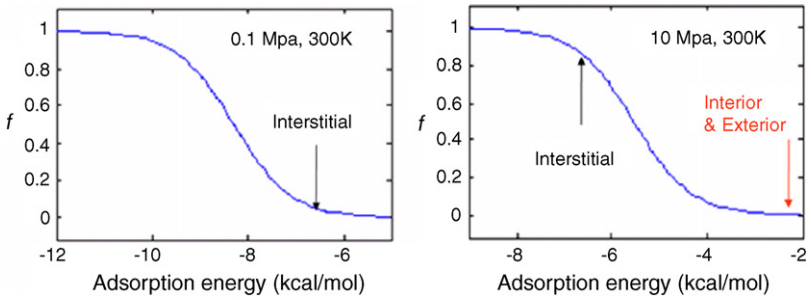

Fig. 2. The relationship between the hydrogen adsorption coverage (f) and the adsorption energy by Langmuir adsorption at different adsorption pressure.

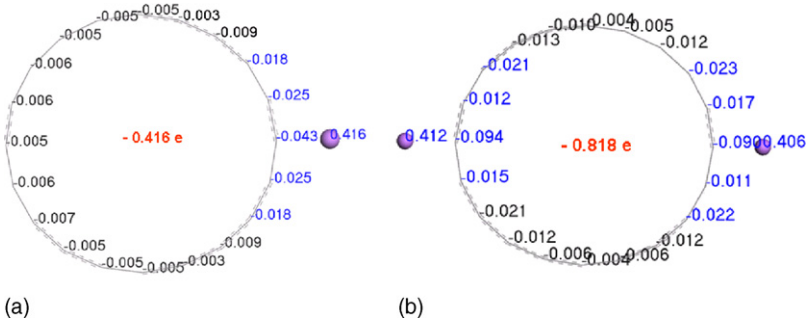

Fig. 4. Mulliken analysis of Li-doped SWCNTs showing the status of electrons transferred from Li atom to SWCNTs; Li/C = 1:40 (a) and Li/C = 1:20 (b).

within small areas. The amount of the electrons transferred increases proportionally with the doping ratio of Li atoms at approximately 0.4 electrons per Li atom.

3.3. Hydrogen storage behavior of Li-doped SWCNTs

We tried to find the effects of Li-doping on the hydrogen adsorption behavior of Li-SWCNTs. The calculations of the adsorption energies indicated that two distinct adsorption sites are created by the doped Li atoms as shown in Fig. 5: one is the region where the distribution status of electrons is influenced by the doped Li atoms (denoted 'region 1') and the other one is the region of positively charged Li atoms, created due to the transfer of electrons from Li atoms to SWCNTs (denoted 'region 2').

Fig. 6 shows that the adsorption energy in region 1 is slightly higher by 0.4 kcal/mol than that of the pristine SWCNTs. As the doping ratio of Li atom increases, the energy also increases slightly. This seems to result from the variation in the electron density due to the doped Li atoms. Indeed, if the electrons are transferred from the doped Li atom to SWCNTs, then SWCNTs becomes negatively charged. A local dipole can subsequently be formed on SWCNTs, which can then induce a dipole on the molecular hydrogen. These dipole/induced dipole and induced dipole/induced dipole interactions between negatively charged SWCNTs and hydrogen molecules reinforce the adsorption energy between SWCNTs and hydrogen molecules. However, Langmuir coverage in region 1 is still below 0.1 so that the hydrogen adsorption capacity will not be greater than that of the pristine SWCNTs. On the other hand, in region 2, which is near to the charged Li atom, the adsorption energy increases considerably by −4.53 to −4.78 kcal/mol. The number of absorbable hydrogen molecules per single Li atom is influenced by a steric effect between hydrogen molecules and by the geometry of nanotube bundles. At least three hydrogen molecules can be adsorbed on one positively charged Li atom. When more hydrogen molecules are adsorbed in region 2, the adsorption energies will vary as shown in Table 1. When two hydrogen molecules are adsorbed by one positively charged Li atom, the adsorption energy is −5.69 kcal/mol and the Langmuir coverage is about 0.55 at 10 MPa and 300 K. Therefore, on this condition an average of 1.1 hydrogen molecules can be stored by one charged Li atom. Because the adsorption energy between pure Li atom and hydrogen molecules was, however, ca. −2.35 to −3.13 kcal/mol in various configurations, we can see that the positively charged Li atom in Li-SWCNTs has a greater capacity to interact with more hydrogen molecules.

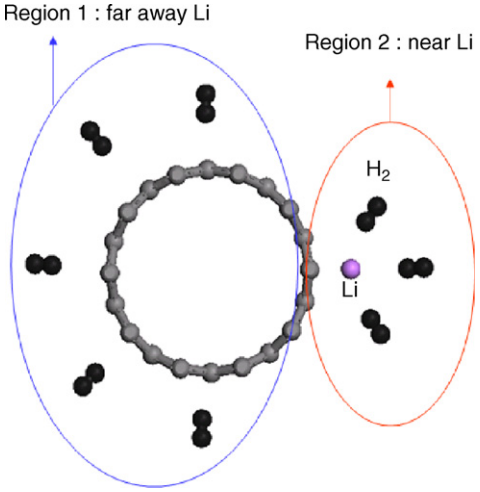

Fig. 5. The structural model showing the two newly created possible adsorption sites in Li-doped SWCNTs.

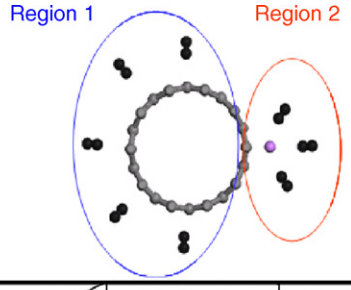

	Region 1 (kcal/mol)	Region 2 (kcal/mol)
0.83 at%	-2.62	-4.68
1.25 at%	-2.66	-4.53
2.5 at%	-2.65	-4.78
5 at%	-2.81	-4.55

Fig. 6. Hydrogen adsorption energy for each adsorption sites in Li-doped SWCNTs as a function of the atomic doping ratio of Li atoms.

Table 1
The variation of the adsorption energy with the number of H_2 molecules adsorbed on Li atom

The number of H_2 molecules	Adsorption energy (kcal/mol)	Corresponding coverage	Average H_2 per Li atom
1	−4.70	0.20	0.2
2	−5.69	0.55	1.1
3	−4.10	0.10	0.3
4	+0.22	–	–

In terms of Langmuir adsorption coverage, the hydrogen adsorption in region 1 of Li-SWCNTs is not better than that of the pristine SWCNTs. This clearly indicates that the enhanced hydrogen storage capacity of the Li-SWCNTs, experimentally reported by earlier studies [12–14], may be due to the additional adsorption by positively charged Li atoms in region 2.

3.4. Hydrogen storage capacity of Li-SWCNTs

To calculate the hydrogen storage capacity in region 1, we established a simple model shown in Fig. 7 and evaluated the effective specific surface area of (10,0) a SWCNT. The dotted line defines the effective specific surface area available on SWCNT. In this model, H_2 molecules were assumed to be absorbed perpendicularly onto the sidewalls of the nanotube because that configuration is more favorable energetically in our preliminarily calculations. The calculations showed that the equilibrium distance between nanotube walls and hydrogen molecules is 0.28 nm and the covalently bonded H–H distance is 0.075 nm. The van der Waals radius of carbon atom is 0.17 nm, so the effective diameter of hydrogen molecule can be said to be 0.295 nm. Using these parameters we got the effective specific surface areas as listed in Table 2 as a function of the number of bundles. The maximum hydrogen storage capacity of (10,0) SWCNTs was calculated from Eq. (3) on the assumption that monolayer physisorption is true:

$$c\,(\mathrm{wt}\%) = \frac{1}{(S_{H_2}/S_{\mathrm{SWCNT}} \times N_A/M_{H_2}) + 1} \quad (3)$$

here, S_{H_2} is the surface area occupied by one H_2 molecule, S_{SWCNT} the total surface area of SWCNTs, N_A the Avogadro number, and M_{H_2} is the mass of a H_2 molecule. To calculate

Table 2
Specific area and H_2 storage capacities on region 1 of Li-doped SWCNTs as a function of the number of individual SWCNTs in a bundle

The number of nanotubes in bundle	Specific surface area (m_2/g)	Theoretical maximum hydrogen capacity (wt%)	H_2 storage capacity at 300 K, 10 MPa (wt%)
1	2664	10.6	0.102
3	1439	6.0	0.058
7	1165	4.9	0.047
19	808	3.5	0.034
37	655	2.8	0.027
61	571	2.5	0.024

S_{H_2}, we assumed that the spheres had a diameter of 0.295 nm, which has a volume equivalent to the hydrodynamic volume of hydrogen molecules, and were closely packed to the surface of SWCNTs.

Considering the Langmuir coverage (f) at room temperature and the pressures in the range of 1–100 MPa together with the maximum storage capacity (c), we then can calculate the hydrogen storage capacities in any specific condition, e.g. room temperature and 10 MPa pressure conditions, by simply multiplying both parameters with each other. The results listed in Table 2 agree well with other data obtained from GCMC simulations and experiments at various temperatures and pressures [23,24]. As SWCNTs usually exist in the form of a bundles containing between a few to a hundred individual tubes, the specific surface area of such bundled SWCNTs varies with the number of nanotubes involved in each bundle. Indeed, Table 2 shows that the effective specific area decreases drastically with increasing the number of nanotubes in each bundle. So, even in the extreme cases, i.e. completely isolated SWCNTs, the hydrogen molecules can be adsorbed at maximum of 0.1 wt% in region 1.

In the case of region 2 we already know that one doped Li atom can accommodate 1.1 hydrogen molecules on average, on the basis of the maximum Langmuir coverage of 0.55. Taking this into account, we calculated the hydrogen storage capacities of Li-doped SWCNTs with the doping ratio of LiC_{15}, which was selected simply because the doping ratio is similar to that observed in the previous experimental works [4,5]. Fig. 8

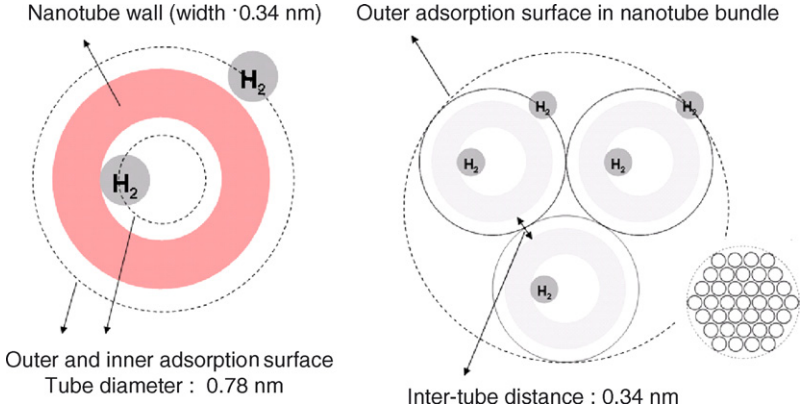

Fig. 7. Simple model for calculation of adsorption surface area.

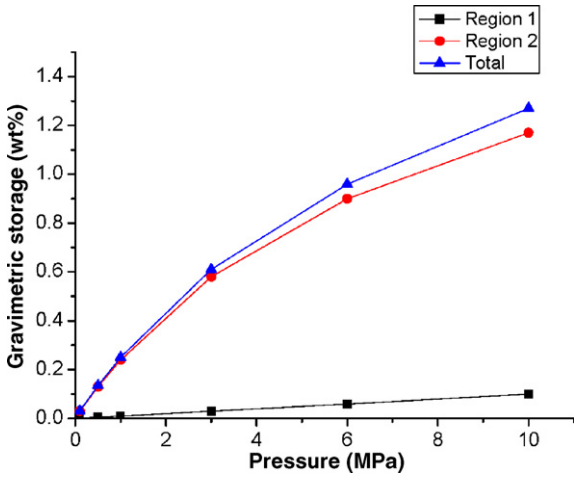

Fig. 8. Hydrogen adsorption capacities of Li-doped (10, 0) SWCNTs at room temperature as a function of storage pressure; region 1 (square), region 2 (circle) and total (triangle).

illustrates the hydrogen adsorption capacity of Li-SWCNTs with the ratio of LiC_{15} as a function of storage pressures. It can be seen that the hydrogen uptake at 300 K and 10 MPa is 0.1 wt% in region 1 and 1.17 wt% in region 2, and that the total hydrogen storage capacity of Li-doped SWCNTs turned out to be 1.27 wt%. This result is somewhat lower than the experimentally reported value, but considering the assumptions made for the Langmuir coverage this value is well within the range of comparable experimental values.

4. Conclusions

It was found from the first principal calculations using DFT that Li-doped SWCNTs have two more adsorption sites (or regions) in addition to the three inherent sites of pristine SWCNTs: 'region 1' is the region where the electron distribution status is influenced by the doped Li atoms and 'region 2' is the region of positively charged Li atoms created by the transfer of electrons from Li atoms to SWCNTs. The adsorption coverage in region 1 at moderate temperature and pressures is not different from that of pristine SWCNTs, although its adsorption energy is slightly higher than that of pristine SWCNTs. However, the adsorption energy in region 2 is approximately two times greater than that of pristine SWCNTs. In addition, at least three hydrogen molecules can be adsorbed on one charged Li atom in region 2. Based on the Langmuir coverage, an average of 1.1 hydrogen molecules can be adsorbed by one charged Li atom at 10 MPa and room temperature. Consequently, the practical reasons of the increase in hydrogen adsorption capacity by Li doping were reasoned to be the enhanced interaction energy and the increased adsorption by the charged Li atom in region 2.

In this study, we did not consider the effects of the intercalation and changes in geometry that might happen as a result of the doping of alkali metals. A further study may be needed to consider those factors.

Acknowledgements

This work was supported financially by the Korea Science and Engineering Foundation (KOSEF) through the Hyper-structured Organic Materials Research Center (HOMRC) at Seoul National University (SNU).

References

[1] M. Hirscher, M. Becher, M. Haluska, U. Dettlaff-Weglikowska, A. Quintel, G.S. Duesberg, Y.-M. Choi, P. Downes, M. Hulman, S. Roth, I. Stepanek, P.B. Hirscher, Appl. Phys. A 72 (2001) 129.
[2] A.C. Dillon, K.M. Jones, T.A. Bekkedahl, C.H. Kiang, D.S. Bethune, M.J. Heben, Nature 386 (1997) 377.
[3] A. Lan, A. Mukasyan, J. Phys. Chem. B 109 (2005) 16011.
[4] J. Li, T. Furuta, H. Goto, T. Ohashi, Y. Fujiwara, S. Yip, J. Chem. Phys. 119 (2003) 2376.
[5] Y. Ye, C.C. Ahn, C. Witham, B. Fultz, J. Liu, A.G. Rinzler, D. Colbert, K.A. Smith, R.E. Smalley, Appl. Phys. Lett. 74 (1999) 2307.
[6] R. Bacsa, C. Laurent, R. Morishima, H. Suzuki, M. Le Lay, J. Phys. Chem. B 108 (2004) 12718.
[7] F. Liu, X. Zhang, J. Chenga, J. Tua, F. Konga, W. Huang, C. Chen, Carbon 41 (2003) 2527.
[8] D. Luxembourg, G. Flamant, A. Guillot, D. Laplaze, Mat. Sci. Eng. B 108 (2004) 114.
[9] M.R. Smith Jr., E.W. Bittner, W. Shi, J.K. Johnson, B.C. Bockrath, J. Phys. Chem. B 107 (2003) 3752.
[10] X. Zhang, D. Cao, J. Chen, J. Phys. Chem. B 107 (2003) 4942.
[11] V.V. Simonyan, J.K. Johnson, J. Alloy. Compd. 330–332 (2002) 659–665.
[12] P. Chen, X. Wu, J. Lin, K.L. Tan, Science 285 (1999) 91.
[13] R.T. Yang, Carbon 38 (2000) 623.
[14] F. Pinkerton, B. Wickle, C. Olk, G. Tibbetts, G. Meisner, M.S. Meyer, J. Herbst, in: Proceedings of the 10th Canadian Hydrogen Conference, Quebec, Canadian Hydrogen Association, 2000.
[15] George E. Froudakis, Nano letters 1 (2001) 531.
[16] I. Cabria, M.J. López, J.A. Alonso, J. Chem. Phys. 123 (2005) 204721.
[17] W. Deng, X. Xu, W.A. Goddard, Phys. Rev. Lett. 92 (2004) 166103.
[18] J.P. Perdew, Y. Wang, Phys. Rev. B 45 (1992) 13244.
[19] B.J. Delley, Chem. Phys. 92 (1990) 508.
[20] $Dmol^3$ in Materials Studio v4.0, Accelrys (USA).
[21] M. Shiraishi, T. Takenobu, H. Kataura, M. Ata, Appl. Phys. A 78 (2004) 947.
[22] F. London, Z. Physik. 63 (1930) 245;
F. London, Z. Physik. Chem. 11 (1930) 222.
[23] M. Rzepka, P. Lamp, M.A. De la Casa-Lillo, J. Phys. Chem. B 102 (1998) 10894.
[24] K.A. Williams, P.C. Eklund, Chem. Phys. Lett. 320 (2000) 352.